LATEST RESULTS OF DIFFRACTIVE AND EXCLUSIVE MEASUREMENTS WITH CMS*

Alexander Bylinkin

for the CMS Collaboration

The University of Kansas, Lawrence, KS, USA

(Received March 7, 2019)

Exclusive $\rho^0(770)$ photoproduction is studied for the first time in ultra-peripheral pPb collisions at $\sqrt{s_{NN}} = 5.02$ TeV. The cross section, $\sigma(\gamma p \to \rho^0(770)p)$, is measured for photon–proton centre-of-mass energies, $W_{\gamma p}$, between 29 and 213 GeV with the CMS experiment. The results are compared to previous measurements and theoretical predictions. The measured cross section $\sigma(\gamma p \to \rho^0(770)p)$ has a power-law energy dependence, consistent with the electron–proton collision measurements performed at HERA.

DOI:10.5506/APhysPolBSupp.12.935

1. Introduction

The CMS detector provides a very wide range of opportunities to study high-energy photon-induced interactions with proton and/or ion beams, due to the high energy and large integrated luminosities available at the LHC. Different exclusive particle production processes at high energies have been studied [1–3]. With the exclusive production of vector meson, parton distribution function at very low-x can be studied. The measurement of exclusive photoproduction of $\rho^0(770)$ mesons in the $\pi^+\pi^-$ decay channel in ultra-peripheral pPb collisions at $\sqrt{s_{NN}} = 5.02$ TeV is presented here.

2. Event selection

Events were selected online by requiring the simultaneous presence of the two beams at the interaction point in conjunction with at least one track in the pixel tracker. Offline, events with the largest energy deposition in any of the HF (hadron forward) towers above the noise threshold of 3 GeV are vetoed. Events are also required to have exactly two tracks corresponding to oppositely charged particles.

---

* Presented at the Diffraction and Low-x 2018 Workshop, August 26–September 1, 2018, Reggio Calabria, Italy.

3. Backgrounds

A large background is due to proton-dissociative events, $\gamma p \to \rho^0(770)p^*$, where p^* is a low-mass hadronic state. The $\rho^0(770)$ is detected while the low-mass state usually escapes undetected by the central region. This contribution is suppressed by rejecting events with activity in the forward calorimeters. In order to determine the residual contribution, a sample of dissociative events is selected by requiring activity in at least one of the forward detectors. This sample provides a template of the $p_{\mathrm{T}}^{\pi^+\pi^-}$ distribution of the dissociative events.

Another sizeable background comes from the exclusive photoproduction of $\rho(1700)$ mesons. The $\rho(1700)$ decays mostly into a $\rho^0(770)$ meson and a pion pair, leading to final states with four charged pions, or with two charged and two neutral pions. It can mimic large $|t|$ $\rho^0(770)$ events, when only two opposite-sign pions escape detection inducing a p_{T} imbalance in the event and thus a distortion in the $|t|$ distribution. The template for this background is estimated using both data and MC samples.

4. Signal extraction

The extraction of the signal contribution is carried out in two steps. First, the proton dissociative and the $\rho(1700)$ contributions are estimated by performing a fit to the data as a function of $p_{\mathrm{T}}^{\pi^+\pi^-}$. This method relies on the fact that exclusive $\rho^0(770)$ events mainly contribute to the low-$p_{\mathrm{T}}^{\pi^+\pi^-}$ region, non-exclusive events dominate the high-$p_{\mathrm{T}}^{\pi^+\pi^-}$ tail, while the $\rho(1700)$ contribution is at intermediate $p_{\mathrm{T}}^{\pi^+\pi^-}$ values. This makes the extraction of the proton dissociative and the $\rho(1700)$ contributions robust. The result of the fit of the $p_{\mathrm{T}}^{\pi^+\pi^-}$ distributions is shown in Fig. 1. The resulting residual proton-dissociative and $\rho(1700)$ contributions, over the whole rapidity interval, are $18 \pm 2\%$ and $20 \pm 2\%$, respectively.

After subtracting these backgrounds, the invariant mass distribution is unfolded using the iterative D'Agostini method [4], which is regularized by four iterations. This procedure leads to corrections for experimental effects including possible data migration between bins. The response matrix is obtained from STARlight.

The invariant mass shape of the ρ^0 in photoproduction is then fitted to the Söding formula [5]

$$\frac{\mathrm{d}N_{\pi^+\pi^-}}{\mathrm{d}M_{\pi^+\pi^-}} = \left| A \frac{\sqrt{M_{\pi^+\pi^-} M_\rho \Gamma(M_{\pi^+\pi^-})}}{M^2_{\pi^+\pi^-} - M^2_{\rho^0} + iM_{\rho^0}\Gamma(M_{\pi^+\pi^-})} + B \right|^2 , \tag{1}$$

where A is the amplitude of the Breit–Wigner function and B is the amplitude of the direct non-resonant $\pi^+\pi^-$ production.

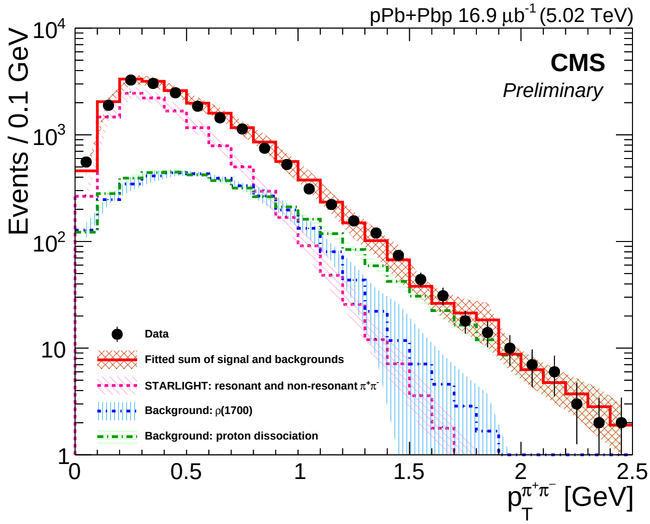

Fig. 1. Template fit to the reconstructed $p_{\rm T}$ of $\pi^+\pi^-$ distribution [1].

Figure 2 shows the fit of the unfolded distribution, which gives $M_{\rho^0} = 776 \pm 1\,(\text{stat.})$ MeV and $\Gamma_{\rho^0} = 154 \pm 3\,(\text{stat.})$ MeV, consistent with the world average values [6]. The ratio of the non-resonant-to-resonant contributions, $|B/A|$, is $0.50 \pm 0.05\,(\text{stat.})$, lower than $0.57 \pm 0.09\,(\text{stat.})$ and $0.70 \pm 0.04\,(\text{stat.})$, the values reported by the H1 and ZEUS collaborations, respectively [7, 8]. Since the ZEUS Collaboration found that $|B/A|$ de-

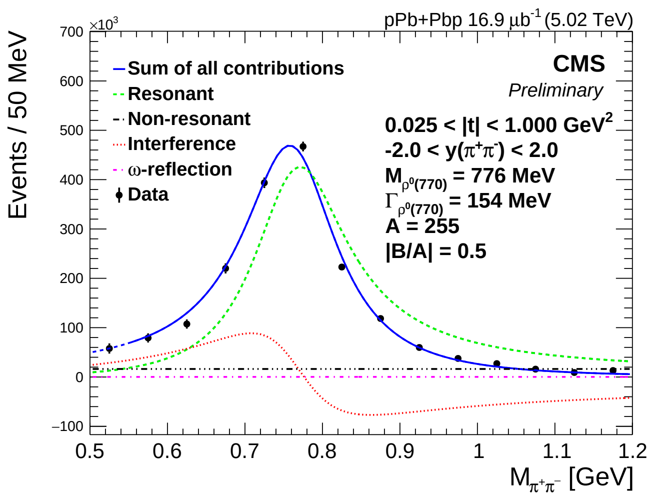

Fig. 2. Invariant mass $M_{\rm inv}(\pi^+\pi^-)$ distribution for ρ^0 [1] in the rapidity interval $|y| < 2.0$ fitted with the Söding model (1).

creases as $|t|$ increases, the fit is repeated for $|t| < 0.5$ GeV^2 resulting in $0.56 \pm 0.06\,(\text{stat.})$, compatible with the HERA results. In addition, no significant dependence of this ratio on $W_{\gamma p}$ is found, in agreement with results reported by ZEUS.

5. Cross section

The differential cross section for exclusive photoproduction is given by

$$\frac{\mathrm{d}\sigma}{\mathrm{d}y} = \frac{N^{\text{exc}}_{\rho^0}}{\mathcal{B} L \Delta y}\,, \tag{2}$$

where $N^{\text{exc}}_{\rho^0}$ is the corrected number of exclusive ρ^0 events obtained from the fits; $\mathcal{B}$ is the branching fraction, equal about 0.99 [6], Δy is the rapidity interval, and L is the integrated luminosity of the data sample. The cross section $\frac{\mathrm{d}\sigma}{\mathrm{d}y}(p\text{Pb} \to p\text{Pb}\rho^0)$ is related to the photon–proton cross section, $\sigma(\gamma p \to \rho^0 p) \equiv \sigma(W_{\gamma p})$, through the photon flux, $\frac{\mathrm{d}n}{\mathrm{d}k}$

$$\frac{\mathrm{d}\sigma}{\mathrm{d}y}\left(p\text{Pb} \to p\text{Pb}\rho^0\right) = k\frac{\mathrm{d}n}{\mathrm{d}k}\sigma\left(\gamma p \to \rho^0 p\right)\,. \tag{3}$$

Here, k is the photon energy, which is determined from the ρ^0 mass and rapidity, according to the formula $k = (1/2)M_{\rho^0}\exp\left(-y_{\rho^0}\right)$. The average photon flux and the average centre-of-mass energy ($\langle W_{\gamma p}\rangle$) values in each rapidity interval are calculated using STARlight.

The resulting photon–proton cross section, obtained for $W_{\gamma p}$ between 29 and 213 GeV ($\langle W_{\gamma p}\rangle = 92.6$ GeV) and integrated over the range $0 < |t| < 0.5$ GeV^2, is $\sigma = 11.2 \pm 1.4\,(\text{stat.}) \pm 1.0\,(\text{syst.})$ μb. The photon–proton cross section values, $\sigma(\gamma p \to \rho^0 p)$, for all rapidity bins are presented in Fig. 3. Figure 3 also shows a compilation of the fixed-target [9–12] and HERA results [7, 8]. The line indicates the result of a fit to all the plotted data with the formula $\sigma = \alpha_1 W_{\gamma p}^{\delta_1} + \alpha_2 W_{\gamma p}^{\delta_2}$. The fit describes the data well. The CMS and HERA data are also fitted with the function $\sigma = \alpha W_{\gamma p}^{\delta}$. The fit yields $\delta = 0.23 \pm 0.14\,(\text{stat.}) \pm 0.04\,(\text{syst.})$.

The unfolded invariant mass distribution is studied for different $|t|$ bins, and the extraction of the ρ^0 photoproduction cross section is repeated in each bin. In order to compare with the HERA results, the p_{T}-related measurements are presented in terms of $|t|$, approximated as $|t| \approx (p_{\mathrm{T}}^{\pi^+\pi^-})^2$.

Figure 4 shows the differential cross section $\mathrm{d}\sigma/\mathrm{d}|t|$ in the rapidity interval $-1.2 < y(\pi^+\pi^-) < 0$, corresponding to a $W_{\gamma p}$ range similar to that at HERA, compared with the H1 and ZEUS results [7, 8]. The Regge formula [13] $b = b_0 + 2\alpha' \ln(\frac{W_{\gamma p}}{W_0})^2$, which parametrizes the dependence of

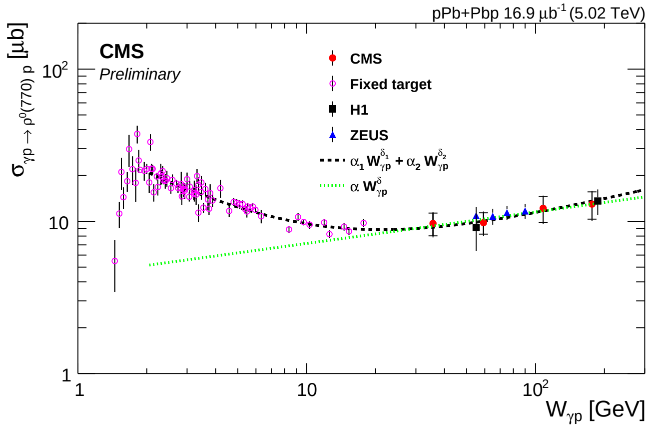

Fig. 3. The total cross section σ of ρ^0 photoproduction [1] as a function of $W_{\gamma p}$.

the exponential slope b of the differential cross section on the collisions energy. The fit to the CMS data alone gives a Pomeron slope $\alpha' = 0.48 \pm 0.33\,(\mathrm{stat.}) \pm 0.12\,(\mathrm{syst.})$ GeV^{-2}, consistent with the ZEUS [8] value and the Regge expectation of 0.25 GeV^{-2}.

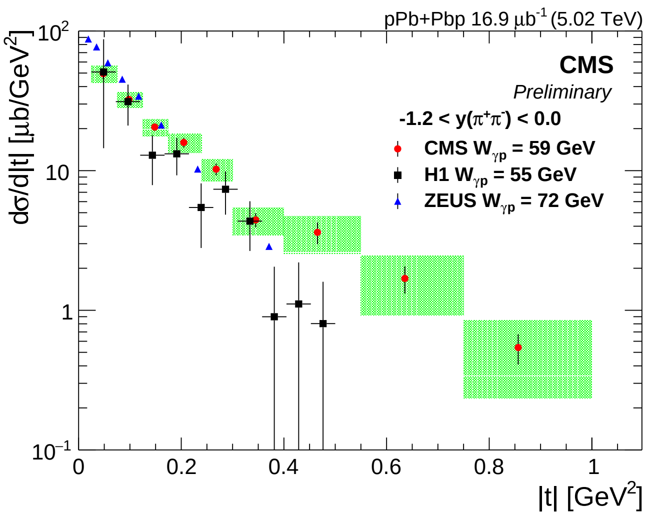

Fig. 4. Differential cross section $\mathrm{d}\sigma/\mathrm{d}|t|$ for exclusive ρ^0 photoproduction [1] in the rapidity interval $-1.2 < y(\pi^+\pi^-) < 0$ together with H1 and ZEUS data [7, 8].

6. Summary

In summary, the CMS Collaboration has made the first LHC measurement of the exclusive ρ^0 photoproduction off protons in UPC pPb collisions at $\sqrt{s_{NN}} = 5.02$ TeV. The cross section of this process is measured in the photon–proton centre-of-mass energy interval $29 < W_{\gamma p} < 213$ GeV. The results are consistent with those of the H1 and ZEUS collaborations. The combination of the present data and the earlier, lower energy results is in good agreement with theoretically inspired fits. The differential cross section $\mathrm{d}\sigma/\mathrm{d}|t|$ for ρ^0 photoproduction is measured as a function of $W_{\gamma p}$.

REFERENCES

[1] CMS Collaboration, https://cds.cern.ch/record/2636688, CMS-PAS-FSQ-16-007.

[2] B.B. Abelev *et al.* [ALICE Collaboration], *Phys. Rev. Lett.* **113**, 232504 (2014) [arXiv:1406.7819 [nucl-ex]].

[3] R. Aaij *et al.* [LHCb Collaboration], *J. High Energy Phys.* **1509**, 084 (2015) [arXiv:1505.08139 [hep-ex]].

[4] G. D'Agostini, *Nucl. Instrum. Methods Phys. Res. A* **362**, 487 (1995).

[5] P. Soding, *Phys. Lett.* **19**, 702 (1966).

[6] C. Patrignani *et al.* [Particle Data Group], *Chin. Phys. C* **40**, 100001 (2016).

[7] S. Aid *et al.* [H1 Collaboration], *Nucl. Phys. B* **463**, 3 (1996) [arXiv:hep-ex/9601004].

[8] J. Breitweg *et al.* [ZEUS Collaboration], *Eur. Phys. J. C* **2**, 247 (1998) [arXiv:hep-ex/9712020].

[9] M.R. Adams *et al.* [E665 Collaboration], *Z. Phys. C* **74**, 237 (1997).

[10] D.G. Cassel *et al.*, *Phys. Rev. D* **24**, 2787 (1981).

[11] C. Hadjidakis *et al.* [CLAS Collaboration], *Phys. Lett. B* **605**, 256 (2005) [arXiv:hep-ex/0408005].

[12] S.A. Morrow *et al.* [CLAS Collaboration], *Eur. Phys. J. A* **39**, 5 (2009) [arXiv:0807.3834 [hep-ex]].

[13] K.A. Goulianos, *Phys. Rep.* **101**, 169 (1983).